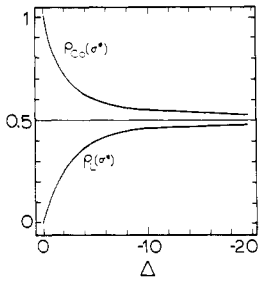

Figure 5. Graph of the values of the orbital coefficients as they vary with Δ. $\rho_{Co}(\sigma^*) = \rho_L(\sigma)$ and $\rho_L(\sigma^*) = \rho_{Co}(\sigma)$ in the absence of overlap. The values were calculated as in ref 13.

of the state of the benzimidazole.

Acknowledgment. The authors wish to thank Edward Deutsch, Hans Jaffe, Darl McDaniel, Graham Palmer, and William Rubinson for critical reading of the manuscript. This work was supported in part by NSF Grant CHE 76-04321.

Appendix

The values of the orbital energies are found by solving the secular determinant, where β defines the generalized interaction and E the eigenvalue energies:

$$\begin{vmatrix} \mathcal{E}-E & \beta-E \\ \beta-E & \mathcal{E}-E \end{vmatrix} = 0$$

We assume no overlap in this model; the conclusions would be unchanged by including it.

We define $\Delta = 2\beta/\mathcal{E}$, where $\mathcal{E}$ is, as depicted in Figure 4, the splitting between the cobalt orbital energy and that of the bound ligand. We denote the electron density contributed by each atomic orbital that goes to make up the two molecular orbitals by, respectively, $\rho_{Co}(\sigma)$, $\rho_L(\sigma)$, $\rho_{Co}(\sigma^*)$, and $\rho_L(\sigma^*)$. The values of the last two are shown graphically as a function of Δ in Figure 5. In the limit of no interaction, $\Delta = 0$, the molecular orbitals become atomic orbitals; $\rho_{Co}(\sigma^*) = \rho_L(\sigma) = 1$ for the system as defined in Figure 4. Further, as the value of Δ takes on larger negative values, the electrons in the orbitals tend increasingly to become equally distributed over the two atomic centers. The orbital coefficients approach 0.5, the value that defines perfect covalency of the bond.

Within the molecular orbital formalism, two ways exist to change the oxidation and reduction potentials of the [Co]cobalamins with changing axial ligation: changing the relative energy splitting between the metal and ligand atomic orbitals, $\mathcal{E}$, and changing the size of the bonding interaction, β. It seems reasonable to consider that the metal orbital remains at a constant energy. Thus, variation in the value of $\mathcal{E}$ will be due only to a change in the different ligand energy levels, which are not experimentally determinable directly. The second possible variation, the magnitude of the bonding interaction, is larger for CH_3 than for H_2O due to the better σ-donor properties of the former.

The first main point of the electrochemistry, concerning the trend in reduction potentials, can be explained by a change in either $\mathcal{E}$ or β. When the cobalt is found, experimentally, to be in a higher formal oxidation state, the theory shows that the antibonding orbital occupied as a result of the reduction must be lower in energy. Both the higher oxidation state and lower σ*-orbital energy results if $2\beta/\mathcal{E}$ becomes smaller. This can occur by either a decrease in β, the bonding interaction, or an increase in $\mathcal{E}$, the atomic orbital energy separation. Thus, the better σ donor will have a higher reduction potential and lower oxidation potential as observed experimentally.

Registry No. Aquocobalamin, 13422-52-1; methylcobalamin, 13422-55-4; coenzyme B_{12}, 13870-90-1.

Contribution from the Department of Chemistry, Purdue University, West Lafayette, Indiana 47907

Electron-Transfer Kinetics between Deprotonated-Peptide Complexes of Nickel(III) and Nickel(II)

CARL K. MURRAY and DALE W. MARGERUM*

Received April 9, 1982

Cross reactions between nickel(III) peptides and nickel(II) peptides in aqueous solution are used to evaluate the self-exchange rate constants, k_{11}, of these species. The values of k_{11} for 16 different peptide complexes vary with their structure but can be classified into the following groups: triply deprotonated peptides (1.2×10^5 M^{-1} s^{-1}), except for $H_{-3}G_5$ (4.2×10^4 M^{-1} s^{-1}), and doubly deprotonated peptides (1.3×10^4 M^{-1} s^{-1}), except for α-aminoisobutyryl tripeptides (5.5×10^2 M^{-1} s^{-1}). The cross reactions are catalyzed by bridging ligands with a 10-fold increase in the rate constant in the presence of 5×10^{-3} M Br^-. The order of enhanced reactivity is $Br^- > Cl^- > N_3^-$, and there is no enhancement with F^-.

Introduction

Nickel(III)–deprotonated-peptide complexes are formed readily from the corresponding nickel(II) species by either electrochemical or chemical oxidation.[1,2] These nickel(III) species are moderately stable in aqueous solution. Their EPR spectra[2,3] and electrochemical behavior[4] are consistent with a tetragonally distorted octahedral structure with two water molecules in the axial sites and the unpaired electron in the metal d_{z^2} orbital. Nitrogen ligands such as pyridine or ammonia have been shown to form axial adducts with nickel(III) peptides.[3,5] On the other hand, the nickel(II) peptides are d^8, square-planar species[4,6] with no axial solvation. Thus, reduction of nickel(III) peptides is accompanied by a release of coordinated water molecules in accord with eq 1, where L

$$Ni^{III}(H_{-n}L)(H_2O)_2 + e^- \rightleftarrows Ni^{II}(H_{-n}L) + 2H_2O \quad (1)$$

is the peptide ligand and n is the number of deprotonated peptide or amide nitrogens in the complex. The $Ni^{III,II}$ reduction potentials vary from 0.79 to almost 0.9 V vs. the normal hydrogen electrode, depending on the nature of the

(1) Bossu, F. P.; Margerum, D. W. *J. Am. Chem. Soc.* **1976**, *98*, 4003.
(2) Bossu, F. P.; Margerum, D. W. *Inorg. Chem.* **1977**, *16*, 1210.
(3) Lappin, A. G.; Murray, C. K.; Margerum, D. W. *Inorg. Chem.* **1978**, *17*, 1630.
(4) Youngblood, M. P.; Margerum, D. W. *Inorg. Chem.* **1980**, *19*, 3068-3072.
(5) Murray, C. K.; Margerum, D. W. *Inorg. Chem.* **1982**, *21*, 3501-3506.
(6) Margerum, D. W.; Dukes, G. R. *Met. Ions. Biol. Syst.* **1974**, *1*, Chapter 5.

0020-1669/83/1322-0463$01.50/0

peptide,[2] so that nickel(III) peptides are moderately strong oxidants in aqueous solution. Relatively little is known, however, about the rates of electron transfer of nickel(III)- and nickel(II)-peptide complexes. The kinetics of reduction by iodide have been studied[7] and found to involve axial coordination of iodide followed by reduction of Ni(III) to Ni(II).

The Marcus theory for outer-sphere electron transfer predicts the relationship in eq 2 for self-exchange rate constants

$$k_{12} = (k_{11}k_{22}K_{12}f)^{1/2}$$
$$\log f = (\log K_{12})^2/[4 \log (k_{11}k_{22}/Z^2)] \quad (2)$$

k_{11} and k_{22}, the equilibrium constant K_{12} for the electron-transfer reaction, and the cross-exchange rate constant k_{12}. Self-exchange rate constants are typically difficult to measure directly since no net reaction occurs. Recently, k_{11} for the copper(III,II)-peptide couple $Cu^{III,II}(H_{-2}Aib_3)^{0,-}$ (Aib = α-aminoisobutyryl) was determined by ^1H NMR line broadening.[8] Cross-reaction rates between different copper-peptide complexes established that the copper(III,II) peptides have approximately equal self-exchange rate constants regardless of the nature of the peptide ligand.

Similar NMR line-broadening experiments were attempted for $Ni^{III,II}(H_{-2}Aib_3)^{0,-}$ mixtures,[9] but the electron-exchange reactions were so slow that no broadening was observed at Ni(III) concentrations less than 10^{-3} M, and higher concentrations caused paramagnetic broadening of the entire spectrum, including the signal of acetone added as a reference. NMR experiments with $Ni^{III,II}(H_{-3}Aib_3a)^{0,-}$ showed broadening at low (10^{-5} M) Ni(III) concentrations, but the observed dependences on Ni(III) and Ni(II) concentrations were complex.

Since the kinetics of the copper(III,II)-peptide cross reactions were successful in establishing k_{11} for those complexes,[8,10] we have measured the rates of a series of cross reactions between nickel(III)- and nickel(II)-peptide complexes. The kinetics of reactions between complexes such as **1**, a tripeptide complex of Ni(III), and **2**, a tetrapeptide

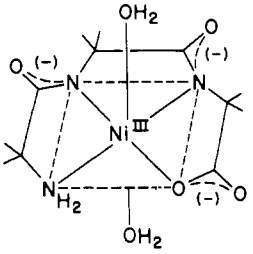

$Ni^{III}(H_{-2}Aib_3)$ (1)

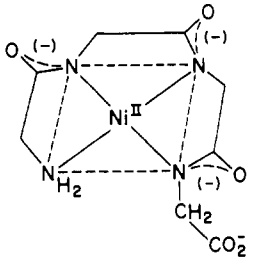

$Ni^{II}(H_{-3}G_4)^{2-}$ (2)

complex of Ni(II), are interpreted in the context of eq 2, and the value of k_{11} is found to vary considerably with the nature of the peptide ligand. In addition, monodentate bridging ligands such as Cl^-, Br^-, or N_3^-, which can coordinate Ni(III) axially, catalyze the electron-exchange reactions via an inner-sphere pathway.

Experimental Section

Materials. The following abbreviations for peptide residues are used: G, glycyl; A, L-alanyl; V, L-valyl; L, L-leucyl; I, L-isoleucyl; Aib, α-aminoisobutyryl. Peptide amides such as glycylglycylglycinamide are denoted as G_3a, etc. The ligand *N,N'*-diglycyl-1,2-diaminoethane is represented as DGEN. The peptides $Aib_3 \cdot 2H_2O$, $A(Aib)_2$ and $Aib_3a \cdot H_2O \cdot CF_3COOH$ were synthesized by A. W. Hamburg with use of methods described elsewhere.[11,12] Other oligopeptides were obtained from Biosynthetika (Oberdorf, Switzerland) or Vega-Fox Chemical Co. DGEN was prepared[13] and isolated as the free base. Pyridine (Fisher Scientific Co.) was purified by vacuum distillation. Solutions of $Ni(ClO_4)_2$ were prepared from the twice-recrystallized salt made by the reaction of $NiCO_3$ and $HClO_4$. All other materials were reagent grade and were used as received. Solutions of nickel(II) peptides were prepared by the reaction of $Ni(ClO_4)_2$ with a 5–15% excess of peptide, adjusted to pH 10. Nickel(III)-peptide complexes were prepared by oxidizing the nickel(II) complex with use of an electrochemical flow system consisting of a graphite-powder working electrode packed in a porous-glass column wrapped externally with a platinum wire.[14] The ionic strength was maintained at 0.1 with $NaClO_4$.

Voltammetry. Equilibrium constants for the electron-transfer reactions were calculated from formal reduction potentials as measured by cyclic voltammetry or differential pulse voltammetry. Electrochemical experiments were carried out with use of a three-electrode system consisting of a glassy-carbon working electrode, a saturated calomel reference electrode, and a platinum wire auxiliary electrode, controlled by either a Bioanalytical Systems CV-1A instrument (cyclic voltammetry) or a Princeton Applied Research Model 174A polarographic analyzer (differential pulse voltammetry). All measurements were carried out at 25.0 ± 0.1 °C.

Stopped-Flow Experiments. Most of the reactions were carried out at pH 7, where decomposition of both nickel(II) and nickel(III) peptides is slow relative to the electron-transfer reaction of interest. In order to minimize decomposition prior to mixing, the nickel(III) solutions were kept in a 0.01 M NaH_2PO_4 medium at pH 5, while the nickel(II) solutions contained 0.01 M Na_2HPO_4 at pH 10. Upon mixing, a buffer at neutral pH was rapidly formed, providing pH control. The reaction of $Ni^{III}(H_{-2}Aib_3)$ with $Ni^{II}(H_{-3}G_4)^{2-}$ also was studied at pH 8.5. In this case, the Ni(II) solution was buffered with 0.05 M borate, and the Ni(III) solution was unbuffered.

In all cases, the reactions were carried out under pseudo-first-order conditions with the Ni(II) reagent in excess. Typically, a nickel(III) tripeptide was used to oxidize a nickel(II) tetrapeptide, tripeptide amide, or other longer chain oligopeptide complex. The reactions were followed by monitoring the absorbance increase at 325 nm for at least 4 half-lives with a Durrum stopped-flow spectrometer interfaced to a Hewlett-Packard Model 2115A or Model 2108 general-purpose computer. At this wavelength, nickel(III) tripeptides (λ_{max} = 345–350 nm, ϵ_{max} = 3800–4700 M^{-1} cm^{-1}) are more transparent than nickel(III) complexes of tetrapeptides or tripeptide amides ($\epsilon_{325} \simeq$ 5200–5700). Typically, absorbance changes were small, on the order of 0.02–0.05 absorbance unit, because of the similarity of the absorbance spectra of the reactants and products. Excellent first-order fits were obtained by linear and nonlinear analysis of the data, giving pseudo-first-order rate constants, k_{obsd}. Plots of k_{obsd} vs. the nickel(II) concentration indicated first-order behavior with respect to the excess reagent as well. This dependence was assumed for those reactions for which no order plot was constructed.

Multilinear analysis of the rate constants was carried out with the Statistical Package for the Social Sciences (SPSS-6000, Version 8.0) on the Purdue CDC 6500 computer system.

Solutions of Nickel Peptide Complexes for NMR. Solutions of $Ni^{II}(H_{-2}Aib_3)^-$ or $Ni^{II}(H_{-3}Aib_3a)^-$ for the NMR experiments were prepared by dissolving the peptide and a 10–15% excess of solid $Ni(ClO_4)_2 \cdot 6H_2O$ in D_2O and then slowly adding NaOD dissolved in D_2O until the fully deprotonated complex was formed at pD $\simeq$ 10–11. Nickel hydroxide precipitate was removed by filtration through a 0.22-μm Millipore filter. The solution was then adjusted to about pD 6.5 and μ = 0.10 by mixing with appropriate quantities of phosphate buffer and $NaClO_4$ in D_2O. Aliquots (0.80 mL) of this solution were transferred to 5-mm NMR tubes.

Nickel(III) solutions were prepared in a manner similar to that for the stopped-flow experiments, except that all solutions were

(7) Raycheba, J. M. T.; Margerum, D. W. *Inorg. Chem.* **1981**, *20*, 1441–1446.
(8) Koval, C. A.; Margerum, D. W. *Inorg. Chem.* **1981**, *20*, 2311–2318.
(9) Murray, C. K. Ph.D. Thesis, Purdue University, 1982.
(10) Anast, J. M.; Hamburg, A. W.; Margerum, D. W., submitted for publication in *Inorg. Chem.*
(11) Kirksey, S. T., Jr.; Neubecker, T. A.; Margerum, D. W. *J. Am. Chem. Soc.* **1979**, *101*, 1631–1633.
(12) Hamburg, A. W.; Kirksey, S. T., Jr.; Margerum, D. W., to be submitted for publication.
(13) Cottrell, T. L.; Gill, J. E. *J. Chem. Soc.* **1947**, 129.
(14) Clark, B. R.; Evans, D. H. *J. Electroanal. Chem.* **1965**, *69*, 181.

Table I. Kinetic Data for Ni(III)/Ni(II) Cross Reactions[a]

	Ni(III) peptide	Ni(II) peptide	$10^4 \times [Ni^{II}]$, M	k_{obsd}, s^{-1}	$10^{-4}k_{12}$, M^{-1} s^{-1}
1.	GGI	G_4	5.00	153 ± 8	30.9 ± 0.4
			4.00	126 ± 6	
			2.00	62 ± 3	
			1.00	31 ± 1	
			0.50	15.5 ± 0.1	
2.	GLG	G_4	6.05	96 ± 5	15.9 ± 0.1
			2.32	36.9 ± 0.7	
			1.22	20.3 ± 0.5	
			0.61	10.0 ± 0.2	
3.	DGEN	G_4	10.60	132 ± 4	12.4 ± 0.3
			5.90	78 ± 2	
			3.01	39.8 ± 0.4	
			0.75	9.9 ± 0.3	
4.	GAG	G_4	10.60	133 ± 5	12 ± 2
			5.90	75 ± 3	
			5.00	51.6 ± 0.5	
			2.09	12.0	
			1.51	21.9	
			1.04	16.3	
5.	GGV	G_4	5.00	132 ± 4	26.4 ± 0.7
6.	GGA	G_4	4.38	63 ± 1	14.4 ± 0.2
7.	A_3	G_4	4.30	36 ± 1	8.4 ± 2
8.	GGV	Aib_3a	4.39	79 ± 2	17.8 ± 0.5
9.	GLG	Aib_3a	4.39	45.7 ± 0.4	10.4 ± 0.1
10.	GAG	Aib_3a	4.39	25.7 ± 0.4	5.9 ± 0.1
11.	G_4a	G_3	50.80	150 ± 3	2.8 ± 0.1
			46.70	133 ± 7	
			31.90	101 ± 2	
			24.90	87 ± 3	
			6.45	23.7 ± 0.2	
			4.26	15.9 ± 0.3	
			2.23	8.6 ± 0.3	
12.	GGI	G_5	5.00	40.5 ± 0.3	8.1 ± 0.3
13.	GLG	G_5	5.00	18.3 ± 0.2	3.67 ± 0.04
14.	GAG	G_5	5.00	11.1 ± 0.2	2.22 ± 0.04
15.	GGV	G_5	5.00	41 ± 1	8.2 ± 0.2
16.	Aib_3	G_4	9.53	13.3 ± 0.3	1.40 ± 0.04
			7.62	10.8 ± 0.3	
			5.72	7.7 ± 0.1	
			2.5[b]	4.4 ± 0.3	
			1.43	2.05 ± 0.04	
17.	Aib_3	G_5	10.00	6.3 ± 0.1	0.63 ± 0.01
			5.00	3.12 ± 0.03	
18.	Aib_3	Aib_3a	12.60	21.9 ± 0.3	1.66 ± 0.07
			6.40	10.9 ± 0.2	
			5.00	6.0 ± 0.1	
			4.57	6.8 ± 0.2	
			4.00	6.5 ± 0.2	
			2.24	3.8 ± 0.2	
			1.28	2.2 ± 0.1	
			0.64	1.24 ± 0.05	
19.	$A(Aib)_2$	Aib_3a	12.60	6.8 ± 0.2	1.6 ± 0.1
			4.57	22.1 ± 0.2	
20.	G_4a	Aib_3	15.00	14.0 ± 0.4	0.91 ± 0.03[c]
			8.00	6.71 ± 0.13	
			6.00	5.56 ± 0.09	
			4.00	3.30 ± 0.06	
			2.00	2.0 ± 0.2	
21.	Aib_3a	Aib_3	10.56	6.7 ± 0.2	0.62 ± 0.03
			5.61	3.34 ± 0.06	
			3.37	1.95 ± 0.03	
22.	GGV	VGG	5.00	14 ± 2	2.8 ± 0.4
23.	GGV	GAG	10.00	36 ± 3	3.5 ± 0.1
			5.00	16.6 ± 0.4	
24.	Aib_3a	G_5	15.00	121 ± 7	8.0 ± 0.1
			10.00	84 ± 4	
			5.00	38 ± 2	
25.	GGV	Aib_3	5.39	4.12 ± 0.07	0.76 ± 0.01

[a] $[Ni^{III}] = (2 \times 10^{-6})$-$(1 \times 10^{-5})$ M; $[PO_4]_T = 0.01$ M; $\mu = 0.1$ $NaClO_4$; pH 7.1 except where noted. [b] pH 8.9 buffered with 0.01 M borate. [c] Owens, G. D. Ph.D. Thesis, Purdue University, 1979.

prepared with D_2O instead of H_2O. The concentrations of all solutions were measured spectrophotometrically.

NMR Spectra. All NMR spectra were recorded with use of a Varian XL-200 FT NMR spectrometer using the signal from HOD as an internal lock. The temperature of the probe was measured by inserting a methanol sample and recording the difference in chemical shift of the two proton resonances.[15] The standard deviation for this measurement is ±0.5 K. Other experimental procedures have been described previously.[8]

Results

Cross Reactions between Ni(III) Peptides and Ni(II) Peptides. The rate constants for 25 cross reactions between a variety of Ni(III) and Ni(II) peptide complexes were determined by the stopped-flow technique. The range of reduction potentials for the nickel(III,II) peptides is rather limited, so only a small range of thermodynamic driving force could be studied. The kientic data are summarized in Table I.

If all the nickel(III,II) complexes had the same self-exchange rate, a plot of log $(k_{12}/f^{1/2})$ vs. log K for the data in Table I would be linear with a slope of 0.5 and an ordinate intercept of log k_{11}. From the plots depicted in Figure 1, it is clear that the above conditions are not met.

For each reaction in Table I, a value of $k_{11}k_{22}$ was calculated by using eq 2 and the $E^{\circ\prime}$ values in Table II. The values of f and $(k_{11}k_{22})^{1/2}$ were calculated iteratively until successive approximations agreed within 1%. Multilinear analysis of these data was carried out to resolve individual k_{11} values. First, the value of k_{11} for each complex was assigned with no assumption that any two k_{11} values were equal. In successive runs, complexes with statistically equal values from the previous run were grouped until values of k_{11} for each set of complexes were statistically distinct. The best fit values are summarized in Table III, and a plot of the logarithm of the observed cross-exchange rate constants, log k_{12}(obsd), against the logarithm of the calculated rate constants, log k_{12}(calcd), is shown in Figure 2.

As indicated in Table III, the apparent self-exchange values were found to be grouped according to the structures of the

Table II. Formal Reduction Potentials of Nickel-Peptide Complexes[a]

peptide	$E^{\circ\prime}$, V	ref	peptide	$E^{\circ\prime}$, V	ref
G_3	0.85	2	Aib_3	0.83	this work
GAG	0.84	this work	$A(Aib)_2$	0.83	this work
GGA	0.85	2	DGEN	0.85	this work
GLG	0.86	2	G_4	0.79	2
GGI	0.89	2	G_3a	0.83	2
GGV	0.89	2	G_4a	0.84	2
VGG	0.85	2	G_5	0.83	2
AAA	0.84	2	Aib_3a	0.815	this work

[a] Determined by cyclic voltammetry or differential pulse voltammetry at a glassy-carbon electrode, $E^{\circ\prime}$ vs. NHE: $\mu = 0.1$ $NaClO_4$; $T = 25$ °C.

Table III. Resolved Apparent Self-Exchange Rate Constants of Ni(III,II) Peptides

peptide	k_{11}, M^{-1} s^{-1}
Aib_3a, G_3a, G_4, G_4a	$(1.2 \pm 0.2) \times 10^5$
G_5	$(4.2 \pm 0.6) \times 10^4$
G_3, GAG, AGG, A_3, GGV, VGG, GLG, GGI, DGEN	$(1.3 \pm 0.1) \times 10^4$
Aib_3, $A(Aib)_2$	550 ± 90

(15) van Geet, A. L. *Anal. Chem.* **1968**, *40*, 2227.

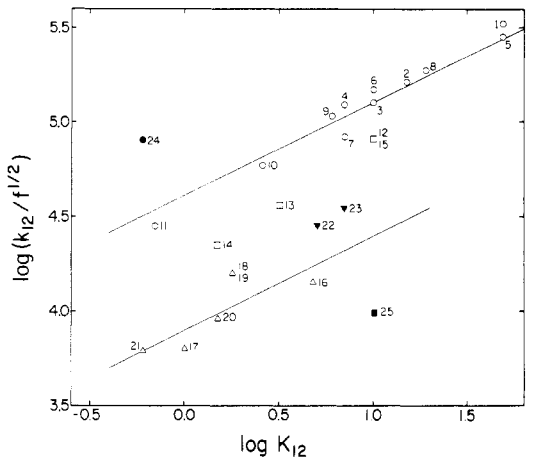

Figure 1. Plot of $k_{12}/f^{1/2}$ vs. log K_{12} for reactions of Ni(III) peptides with Ni(II) peptides at 25.0 °C and μ = 0.1: (○) reactions of doubly deprotonated complexes except those of Aib_3 and $A(Aib)_2$ with triply deprotonated complexes except $Ni^{III,II}(H_{-3}G_5)^{-,2-}$; (△) reactions of $Ni^{III,II}(H_{-2}Aib_3)^{0,-}$ or $Ni^{III,II}(H_{-2}A(Aib)_2)^{0,-}$ with triply deprotonated complexes; (□) reactions of $Ni^{III}(H_{-2}L)$ with $Ni^{II}(H_{-3}G_5)^{2-}$, L ≠ Aib_3 or $A(Aib)_2$; (▼) reactions of $Ni^{III}(H_{-2}GGV)$ with $Ni^{II}(H_{-2}GAG)^-$ and $Ni^{II}(H_{-2}VGG)^-$; (■) reaction of $Ni^{III}(H_{-2}GGV)$ + $Ni^{II}(H_{-2}Aib_3^-)$; (●) reaction of $Ni^{III}(H_{-3}Aib_3a)$ + $Ni^{II}(H_{-3}G_5)^{2-}$. Solid lines are drawn with slope 0.5 through the open circles and open triangles. The points are numbered according to Table I.

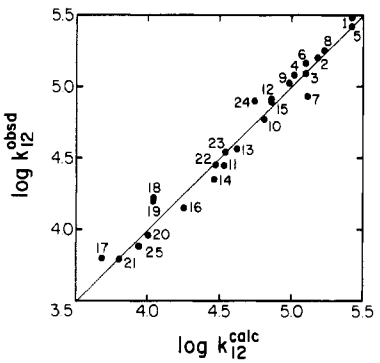

Figure 2. Plot of log k_{12}(obsd) vs. log k_{12}(calcd) using the values of k_{11} in Table III and $E^{\circ\prime}$ in Table II. The solid line has a slope of unity and passes through the origin. The points are numbered according to Table I.

peptide complexes. In Figure 1, the points are divided according to the classifications in Table III. Within each group of reactions, the data behave as predicted by eq 2. The largest groups of complexes studied include the triply deprotonated complexes except $Ni^{III,II}(H_{-3}G_5)^{-,2-}$ and the doubly deprotonated complexes except $Ni^{III,II}(H_{-2}Aib_3)^{0,-}$ and $Ni^{III,II}(H_{-2}AAib_2)^{0,-}$. The triply deprotonated complexes have one amine nitrogen and three deprotonated peptide or amide nitrogens in a square-planar arrangement about the metal, while the tripeptide complexes have an amine nitrogen, two deprotonated peptide nitrogens, and a carboxylate oxygen bound to the nickel ion. The complex of pentaglycine (G_5) has the possibility of axial coordination of the terminal carboxylate group, so that all the groups in Table III except the last (containing $Ni^{III,II}(H_{-2}Aib_3)^{0,-}$) have differences in coordination about the nickel center. The complex of *N,N'*-diglycyl-1,2-diaminoethane (DGEN) has two amine donors and two deprotonated amide donors, but its reactivity is similar to that of the tripeptide complexes. This may be fortuitous, although the EPR spectrum of $Ni^{III}(H_{-2}DGEN)$ closely resembles those of the Ni(III) tripeptides.[3,5] The exceptionally low value of k_{11} for $Ni^{III,II}(H_{-2}Aib_3)^{0,-}$ and $Ni^{III,II}(H_{-2}AAib_3)^{0,-}$ will be discussed below.

Table IV. Kinetic Data for Ni(III)/Ni(II) Cross Reactions in the Presence of Coordinating Ligands

Ni(III) peptide	Ni(II) peptide	X	$10^4[Ni^{II}]$, M	$10^3[X]$, M	k_{obsd}, s^{-1}
Aib_3	G_4	Cl^-	5.0	0	7.72 ± 0.03
			5.0	2.66	8.01 ± 0.03
			5.0	9.11	8.63 ± 0.07
			5.0	18.2	9.7 ± 0.1
			5.0	27.3	10.4 ± 0.1
Aib_3	Aib_3a	Cl^-	5.0	0	6.8 ± 0.1
			5.0	10.1	8.23 ± 0.08
			5.0	20.2	9.7 ± 0.1
			5.0	30.3	11.3 ± 0.2
Aib_3	G_4	Br^-	7.56	1.00	23.0 ± 0.7
			7.56	2.00	37.4 ± 0.8
			7.56	3.00	50 ± 1
			7.56	4.00	63 ± 2
			7.56	5.00	76 ± 1
Aib_3	Aib_3a	Br^-	5.0	1.25	25.3 ± 0.3
			5.0	2.50	41.9 ± 0.6
			5.0	3.75	62.3 ± 0.3
			5.0	5.00	79 ± 1
Aib_3	G_3a	Br^-	1.2	0.16	2.03 ± 0.09
			4.0	0.59	9.3 ± 0.4
			4.8	0.65	12.2 ± 0.1
			5.0	0.74	11.8 ± 0.2
			5.0	1.88	24.5 ± 0.3
			5.0	3.13	37.4 ± 0.5
			5.0	4.38	50.4 ± 0.7
			5.0	5.63	62 ± 1
			11.6	1.78	51 ± 1
			16.8	2.29	90 ± 5
			19.3	2.97	129 ± 2
			24.0	3.27	184 ± 5
GAG	G_4	Br^-	5.0	0	51.6 ± 0.5
			5.0	1.00	59 ± 2
			5.0	2.00	64 ± 2
			5.0	3.00	72 ± 2
Aib_3	G_4	N_3^-	5.5	1.14	18.7 ± 0.2
			5.5	2.29	26.2 ± 0.4
			5.5	3.43	32.7 ± 0.6
			5.5	4.57	38.3 ± 0.4
			5.5	8.00	50 ± 2
			5.5	11.4	57 ± 1
			5.5	17.1	65 ± 1
Aib_3	G_4	py	4.3	0	5.99 ± 0.08
			4.3	2.40	5.7 ± 0.1
			4.3	7.20	5.5 ± 0.1
			4.3	24.0	4.96 ± 0.04
			4.3	72.0	4.2 ± 0.2

The apparent self-exchange rate constants are accurate only to the extent that eq 2 reliably predicts cross-exchange rate constants from self-exchange values. It has been pointed out[16,17] that, for many cross reactions, the observed rate constant is less than that predicted by the Marcus theory and that the discrepancy widens with increasing values of K_{12}. The reactions in this study have small driving forces (K_{12} < 50), and considering the structural similarities between the reactants as well as the good fit to eq 2 (Figure 2), we believe these values to be fairly accurate.

Effect of Ligands Capable of Axial Coordination to Ni(III). The cross-exchange reaction rates are affected by the presence of species that can coordinate the nickel(III) complex axially. The reactions are catalyzed by chloride, bromide, and azide ions but are inhibited by pyridine (Table IV). In the cases of chloride and bromide, plots of k_{obsd} vs. halide concentration $[X^-]$ for the reactions in Table IV are linear, consistent with a reaction pathway that is first order in Ni(II), Ni(III), and halide. The effects of azide and pyridine on the rate of oxidation of $Ni^{II}(H_{-3}G_4)^{2-}$ by $Ni^{III}(H_{-2}Aib_3)$ were studied as well. A plot of k_{obsd} vs. ligand concentration [X], where X = pyr-

(16) Chou, M.; Creutz, C.; Sutin, N. *J. Am. Chem. Soc.* **1977**, *99*, 5615.
(17) Weaver, M.; Yee, E. *Inorg. Chem.* **1980**, *19*, 1936–1945.

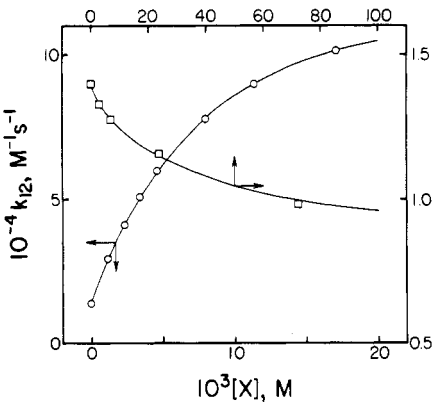

Figure 3. Dependences of the rate of $Ni^{III}(H_{-2}Aib_3) + Ni^{II}(H_{-3}G_4)^{2-} \rightarrow Ni^{II}(H_{-2}Aib_3)^- + Ni^{III}(H_{-3}G_4)^-$ upon pyridine and azide concentrations: (○) X = N_3^-, lower and left axes; (□) X = pyridine, upper and right axes. Solid lines are calculated from the values in Table V.

idine or azide, is depicted in Figure 3. These results are consistent with the mechanism in eq 3–5. Under pseudo-

$$Ni^{III}(H_{-n}L) + X \underset{}{\overset{K_X}{\rightleftharpoons}} Ni^{III}(H_{-n}L)(X) \quad (3)$$

$$Ni^{III}(H_{-n}L) + Ni^{II}(H_{-m}L') \xrightarrow{k_{12}} Ni^{II}(H_{-n}L) + Ni^{III}(H_{-m}L') \quad (4)$$

$$Ni^{III}(H_{-n}L)(X) + Ni^{II}(H_{-m}L') \xrightarrow{k_X} Ni^{II}(H_{-n}L) + Ni^{III}(H_{-m}L') + X \quad (5)$$

first-order conditions in which Ni(II) is in excess, the rate law in eq 6 and 7 results.

$$\frac{d[Ni^{III}(H_{-m}L')]}{dt} = k_{obsd}[Ni^{III}(H_{-n}L)] \quad (6)$$

$$k_{obsd} = \frac{k_{12} + k_X K_X[X]}{1 + K_X[X]}[Ni^{II}(H_{-m}L')] \quad (7)$$

Equilibrium constants for coordination of a number of monodentate ligands have recently been determined.[5] Halide complexes were too weak to be detected even at $[X^-] = 1.0$ M, while the azide and pyridine complexes of $Ni^{III}(H_{-2}Aib_3)$ had stability constants of 137 and 40 M^{-1}, respectively. Hence, when X = Cl^- or Br^-, the value of $K_X[X]$ in eq 7 is small compared to unity and eq 7 reduces to eq 8, where $k_X' = k_X K_X$.

$$k_{obsd} = (k_{12} + k_X'[X])[Ni^{II}(H_{-m}L')] \quad (8)$$

The observed rate constant thus varies linearly with [X]. Values of k_X' calculated from a least-squares analysis of the data in Table IV are summarized in Table V.

As previously mentioned, complexes of Cl^- and Br^- are too weak to detect electrochemically even at 1.0 M concentrations, which implies that K_X in eq 7 is less than 0.2 M^{-1}. With use of this value and the results in Table V, lower limits on k_X, the rate constants for reaction of $Ni^{II}(H_{-3}G_4)^{2-}$ with $Ni^{III}(H_{-2}Aib_3)(X)(H_2O)^-$, can be estimated as $k_{Cl} > 10^6$ M^{-1} s^{-1} and $k_{Br} > 10^8$ M^{-1} s^{-1} for X = Cl^- and Br^-, respectively. In the absence of halide, k_{12} for this reaction is 1.4×10^4 M^{-1} s^{-1}. Thus the rate enhancement compared to that for the aquo species is at least a factor of 70 for chloride and at least a factor of 7000 for bromide.

In the presence of azide or pyridine, the rate constant is not linear with [X], but a limiting rate is approached at high concentrations (Figure 3). Under these conditions, where $K_X[X] >> 1$ and $k_{12} << k_X K_X[X]$, eq 7 reduces to eq 9, and

$$k_{obsd} = k_X[Ni^{II}(H_{-m}L')] \quad (9)$$

the rate constant becomes independent of [X]. The data in Table IV were fit to eq 7 with use of a nonlinear least-squares program, and the values of K_X and k_X thus obtained are summarized in Table V. The values of K_X are in good agreement with those previously reported.[5] For azide, the fully formed axial adduct reacts about 10 times faster than the diaquo complex, and the pyridine complex reacts more slowly that the unsubstituted form by about a factor of 2.

The rate of electron transfer between $Ni^{III}(H_{-2}Aib_3)$ and $Ni^{II}(H_{-3}G_4)^{2-}$ was unaffected by F^-, HPO_4^{2-}, borate, acetate, and OH^- over the pH range 6–8.5. Other bridging ligands such as CN^-, I^-, and SCN^- are rapidly oxidized by nickel(III) peptides, so their utility as electron-transfer catalysts could not be examined.

NMR Line-Broadening Experiments. Attempts were made to measure directly k_{11} for $Ni^{III,II}(H_{-2}Aib_3)^{0,-}$ and $Ni^{III,II}(H_{-3}Aib_3a)$ by ^1H NMR line broadening. At pH 6–7, the decomposition of both oxidation states of these complexes is slow enough for this type of experiment, which requires minimal decomposition over several hours.

The ^1H NMR spectra of the Ni(II) complexes consist of three singlets arising from three pairs of methyl groups on the α-carbons of the peptide. The nickel(III) complexes have no observable spectrum because of paramagnetic broadening. Mixtures of the two oxidation states should give broadened lines due to electron exchange.[8]

In the case of $Ni^{III,II}(H_{-2}Aib_3)^{0,-}$ no broadening was observed even at $[Ni(III)] = 1.2 \times 10^{-3}$ M. With the assumption of a slow-exchange model,[18-20] eq 10 is operative, where fwhm

$$\pi(\text{fwhm} - \text{fwhm}_0) = k_{11}[Ni(III)] \quad (10)$$

denotes the line width of the NMR signal and fwhm_0 is the line width in the absence of Ni(III). The value of fwhm_0 was typically <1.0 Hz, and if it is assumed that broadening of 0.3 Hz is detectable, an upper limit of $k_{11} < 800$ M^{-1} s^{-1} can be set for $Ni^{III,II}(H_{-2}Aib_3)^{0,-}$, consistent with the value of 550 ± 150 M^{-1} s^{-1} calculated from the cross-reaction data.

For $Ni^{III,II}(H_{-3}Aib_3a)^{0,-}$, broadening was observed, but the dependence of the left-hand side of eq 10 upon the concentration of nickel(II) was complex, and the line-broadening behavior could not be described by eq 10. The observed behavior did not follow the criteria for the "fast-exchange" limit[18,20] either, so the experiments were not pursued. The fact that broadening was observed at small Ni(III) concentrations (<10^{-5} M) is evidence that the self-exchange rate of $Ni^{III,II}(H_{-3}Aib_3a)^{0,-}$ is considerably greater than that of $Ni^{III,II}(H_{-2}Aib_3)^{0,-}$.

In a series of experiments in which Br^- or Cl^- was added to mixtures of $Ni^{III}(H_{-2}Aib_3)$ and $Ni^{II}(H_{-2}Aib_3)^-$, broadening of the NMR signal was observed, qualitatively demonstrating

Table V. Resolved Rate and Equilibrium Constants for Ni(III)/Ni(II) Electron-Transfer Reactions in the Presence of Coordinating Ligands

Ni(III) peptide	Ni(II) peptide	X	$k_X K_X$, M^{-2} s^{-1}
Aib_3	G_4	Cl^-	$(2.0 \pm 0.1) \times 10^5$
Aib_3	Aib_3a	Cl^-	$(2.90 \pm 0.05) \times 10^5$
Aib_3	G_4	Br^-	$(1.73 \pm 0.06) \times 10^7$
Aib_3	G_3a	Br^-	$(2.0 \pm 0.1) \times 10^7$
Aib_3	Aib_3a	Br^-	$(2.90 \pm 0.05) \times 10^7$
GAG	Aib_3a	Br^-	$(2.1 \pm 0.2) \times 10^7$
GAG	G_4	Br^-	$(1.34 \pm 0.06) \times 10^7$

Ni(III) peptide	Ni(II) peptide	X	k_X, M^{-1} s^{-1}	K_X, M^{-1}
Aib_3	G_4	N_3^-	$(1.71 \pm 0.03) \times 10^5$	115 ± 5
Aib_3	G_4	py	$(8 \pm 1) \times 10^3$	28 ± 11

(18) Dietrich, M. W.; Wahl, A. C. *J. Chem. Phys.* **1963**, *38*, 1591.
(19) Swift, T. J.; Connick, R. E. *J. Chem. Phys.* **1962**, *37*, 307.
(20) Leigh, J. S., Jr. *J. Magn. Reson.* **1971**, *4*, 308–311.

that the self-exchange rates are affected in a manner similar to that for the cross-reaction rates.

Discussion

Nickel(III,II) Self-Exchange Rate Constants. The self-exchange rate constants for copper(III,II)–peptide complexes have recently been reported as $(0.9–5.5) \times 10^4$ M^{-1} s^{-1} at 25.0 °C.[8,10] These values are fairly independent of the nature of the peptide ligand; i.e., tripeptide and tetrapeptide complexes have about the same self-exchange rate constant, even though the donor groups to the metal differ. Furthermore, the Aib_3 complex, with two methyl groups on each α-carbon, has a self-exchange rate slightly greater than that of $Cu^{III,II}(H_{-3}Aib_3a)^{0,-}$ or $Cu^{III,II}(H_{-3}G_4)^{-,2-}$.[10]

For the nickel peptides, the present data indicate that the value of k_{11} varies with the donor groups coordinated to the metal. The magnitude of k_{11} for most of the tripeptide complexes differs from that of the triply deprotonated complexes by about a factor of 10, but with the exceptions of $Ni^{III,II}(H_{-2}Aib_3)^{0,-}$, and $Ni^{III,II}(H_{-2}AAib_2)^{0,-}$, the apparent self-exchange rate constants for the nickel complexes are not greatly different from the corresponding copper rate constants.

In contrast to the copper peptide results, however, the apparent self-exchange rate constant for $Ni^{III,II}(H_{-2}Aib_3)^{0,-}$ and $Ni^{III,II}(H_{-2}A(Aib)_2)^{0,-}$ is a factor of 20 less than that of the other tripeptide complexes and $\sim$100 times smaller than those of the corresponding Cu(III,II) complexes. Thus while the Cu(III,II) self-exchange rate constants vary by a factor of only about 5, the nickel(III,II) self-exchange rate constants vary by a factor of about 200. The difference in k_{11} values between the triply deprotonated complexes and the complexes of the tripeptides except Aib_3 and $A(Aib)_2$ is a factor of 10, but $Ni^{III,II}(H_{-2}Aib_3)^{0,-}$ and $Ni^{III,II}(H_{-2}AAib_2)^{0,-}$ have self-exchange rate constants 20 times smaller than the other tripeptide complexes. The reason for the relatively sluggish behavior of the Aib-containing tripeptides is not clear. We have considered a variety of explanations, but each has serious drawbacks. Nonetheless, we would like to outline several possibilities.

The intrinsic reactivity of a species with respect to electron transfer is governed by inner- and outer-sphere rearrangements of the reactant which must occur before electron transfer can take place.[21-23] The height of this Franck–Condon barrier is dependent on the local environment of the metal ion and may vary with different inner-sphere donors. Thus, the observed difference in k_{11} between the triply deprotonated nickel(III,II) complexes and the doubly deprotonated complexes is not surprising. More puzzling are the small values of k_{11} for the Aib_3 and $A(Aib)_2$ complexes compared to values for other tripeptide complexes of nickel. The major structural difference of the Aib-containing complexes is the presence of methyl groups both above and below the plane of the complex. These methyl groups do not interfere with axial coordination to the metal.[5] The UV–visible and EPR spectra of the Aib_3 and $A(Aib)_2$ complexes are typical of the other nickel peptides. It is unlikely, therefore, that the methyl groups cause large changes in the rearrangement energy required for electron transfer. If such effects were present, they should also be apparent in the Aib_3a complex, but this species reacts as rapidly as the other triply deprotonated complexes.

Another possible explanation for the sluggishness of the Aib_3 and $A(Aib)_2$ complexes is that, for most of the peptide complexes, there is a favorable intermolecular interaction between nickel(II) and nickel(III) species, which is sterically blocked by the methyl groups in $Ni(H_{-2}Aib_3)^{0,-}$ and $Ni(H_{-2}A(Aib)_2)^{0,-}$. The other tripeptides are composed of L isomers (except glycyl residues) and thus have all the alkyl side chains on one side of the complex, leaving the other side open. $Cu^{III}(H_{-2}Aib_3)$ has been shown to react much more slowly than other copper peptides with nickel(II) peptides, with tris(1,10-phenanthroline)cobalt(II),[8,25] and with bis(2,9-dimethyl-1,10-phenanthroline)copper(I),[8,26] even though the self-exchange rate constants for copper peptides are about equal, implying that steric hindrance may be important in these cases.

At least two types of intermolecular interaction are possible for the nickel peptides. One involves inner-sphere bridging of the axial sites of the two reactants by a water molecule, but water is considered a very poor bridging ligand.[27] A hydroxide bridge may be eliminated because there is no dependence of the reaction rates on pH. A bridging water mechanism cannot be ruled out entirely, however, since halide ions apparently catalyze the reactions by a similar pathway. The lack of an effect for the Aib_3a complex raises problems, since steric blocking of a water bridge should be as significant for this complex as for $Ni^{III,II}(H_{-2}Aib_3)^{0,-}$ or $Ni^{III,II}(H_{-2}A(Aib)_2)^{0,-}$.

Another type of intermolecular interaction involves a preassociation of the nickel(II) and nickel(III) species followed by electron transfer. Such associations are affected by the reactants' size, charge, and hydrophilic–hydrophobic characteristics[28] and a variety of other considerations. Since $Ni^{III,II}(H_{-3}Aib_3a)^{0,-}$ reacts "normally", any proposed mechanism must account for the large differences in behavior between this species and $Ni^{III,II}(H_{-2}Aib_3)^{0,-}$, as established by both the NMR and cross-reaction data. The only difference in the structures is replacement of a carboxylate oxygen in the tripeptide complex with a deprotonated-amide nitrogen in the Aib_3a complex. Furthermore, the methyl groups do not interfere with access to the metal by a small entering group.[5] The functional groups most shielded by the methyl groups are the adjacent deprotonated-peptide nitrogens. For the $A(Aib)_2$ and Aib_3 complexes, both deprotonated-peptide nitrogens are blocked, but in the Aib_3a complex, the terminal amide nitrogen is accessible. In the complexes containing no Aib residues, all the peptide nitrogens are accessible from at least one side of the complex. These considerations suggest that the anomalous behavior of the Aib_3 and $A(Aib)_2$ complexes is related to blocking of the deprotonated-peptide nitrogens in these species.

One way that accessibility of the peptide nitrogens might affect the rate constant involves coordination of a nitrogen of nickel(II) to an axial site of nickel(III). Such an intermolecular interaction between peptides and metal ions is known in crystals of $Na[Cu(H_{-2}G_3)]\cdot H_2O$,[29] and molecular models indicate that this might be possible for $Ni^{III,II}(H_{-3}Aib_3a)^{0,-}$ but not for $Ni^{III,II}(H_{-2}Aib_3)^{0,-}$, in which the peptide nitrogens are sterically blocked. Since the axial sites of $Ni^{III}(H_{-2}Aib_3)$ are accessible, however, this interaction should only be hindered when the Aib_3 or $A(Aib)_2$ complex is the nickel(II) reactant. Experimentally, the effect is observed regardless of whether the Aib_3 or $A(Aib)_2$ complex is the Ni(III) or the Ni(II) reactant. This problem could be overcome by postulating that the Ni(II) ion is simultaneously coordinated by a peptide nitrogen of Ni(III), but such a geometry is not possible for the Aib_3a complex.

Another possibility is that the solvent structure about the amide nitrogens is disrupted when methyl groups are adjacent and that this affects the energy of the axially coordinated

(21) Brown, G. M.; Sutin, N. *J. Am. Chem. Soc.* **1979**, *101*, 883–892.
(22) Marcus, R. A. *J. Chem. Phys.* **1956**, *24*, 966.
(23) Sutin, N. *Annu. Rev. Nucl. Sci.* **1962**, *12*, 285.
(24) Owens, G. D.; Phillips, D. A.; Czarnecki, J. J.; Raycheba, J. M. T.; Margerum, D. W., to be submitted for publication.
(25) DeKorte, J. M.; Owens, G. D.; Margerum, D. W. *Inorg. Chem.* **1979**, *18*, 1538.
(26) Lappin, A. G.; Youngblood, M. P.; Margerum, D. W. *Inorg. Chem.* **1980**, *19*, 407.
(27) Haim, A. *Acc. Chem. Res.* **1975**, *8*, 264–272.
(28) Taube, H. *Adv. Chem. Ser.* **1977**, *No. 162*, 127.
(29) Freeman, H. C. *Adv. Protein Chem.* **1967**, *22*, 331–332, 405.

waters in the transition state. A third alternative is that a nitrogen–nitrogen π interaction can provide a facile route for electron transfer between the metal centers. These interactions, however, have no direct evidence supporting them, and in any case, such effects would probably appear in the copper(III,II) exchange, as well.

One final possibility for the sluggish behavior of the Aib_3 and $A(Aib)_2$ complexes is that these complexes react nonadiabatically. Increased steric bulk is expected to favor nonadiabatic behavior, but the overall size of these complexes is rather small compared to that of many species such as tris(1,10-phenanthroline)iron(III,II), which are believed to fall well within the adiabatic regime.[28] However, recent calculations by Newton[30] indicate that nonadiabaticity may be more common than previously thought, and strong π–π interactions may be responsible for the adiabaticity of the $Fe^{III,II}(phen)_3^{3+,2+}$ self-exchange reaction. In any case, the steric bulk of $Ni^{III,II}(H_{-3}Aib_3a)^{0,-}$ and $Cu^{III,II}(H_{-2}Aib_3)^{0,-}$ is as great as that of $Ni^{III,II}(H_{-2}Aib_3)^{0,-}$, and no effect is observed with these complexes. Thus, while nonadiabaticity cannot be ruled out entirely, it seems to be an unlikely explanation for our results.

It is interesting to compare the effects of ligand structure on both the thermodynamic and kinetic properties of the copper(III,II) peptides and the nickel(III,II) peptides. In the former case, the self-exchange rate constant is relatively independent of the peptide with typical values ranging from 9×10^3 to 5.5×10^4 M^{-1} s^{-1}.[8,10] The Cu(III,II) reduction potential, however, is strongly dependent on the peptide structure, ranging from 0.37 to 0.81 V vs. NHE[10,31] for the complexes studied. On the other hand, the nickel(III,II) potentials cover only the limited range of 0.79 to 0.89 V vs. NHE,[2] but the self-exchange rates can differ by more than a factor of 200.

Catalysis by Bridging Ligands. The observed catalysis of the nickel peptide electron-transfer reactions is consistent with an inner-sphere pathway with halide or azide bridging the axial sites of the two nickel complexes. The rate of the bromide-catalyzed pathway is insensitive to the thermodynamic driving force of the reaction and is insensitive to the resolved self-exchange rate constants of the reactants (Table V), factors that strongly affect the outer-sphere pathway. For example, the rate constants for the Br^- pathway for the reactions in Table V span only about a factor of 2, while the rate constants for the same reactions in the absence of halides differ by a factor of about 10. Furthermore, the direction of the trend in the latter reactions is not followed for the halide pathway.

Axial substitution of a nonbridging ligand (pyridine) reduces the rate of electron transfer. Hence we conclude that Br^-, Cl^-, and N_3^- are behaving as true bridging ligands and that the halide- and azide-catalyzed pathways are genuine inner-sphere mechanisms.

The relative order of reactivity of the bridging ligands is $Br^- > Cl^- > N_3^- >> F^-, CH_3CO_2^-$, the so-called "normal" reactivity pattern. Typically, for electron transfer between e_g orbitals as in this case, the reactivity varies as $Cl^- > N_3^- >> CH_3CO_2^-$,[27] as observed. For transfer from e_g to t_{2g} orbitals, azide is normally a better bridging ligand than chloride. This behavior has been interpreted in terms of the symmetry of the metal and ligand orbitals.[32,33]

Studies with copper(III,II) peptides have demonstrated that there are two pathways for electron transfer.[8,10,34-36] An inner-sphere pathway predominates for reactions with $Ir^{IV,III}Cl_6^{2-,3-}$[34,35] and $Fe(CN)_6^{3-,4-}$,[36] while an outer-sphere pathway is exemplified by reactions of copper(III) peptides with $Ru(NH_3)_6^{2+}$,[10] $Ru(NH_3)_5py^{2+}$,[10] and copper(II) peptides.[8,10] A weak water bridge cannot be ruled out in the latter case, but since the results agree with the results of the $Ru(NH_3)_6^{2+}$ reactions, it is not necessary or desirable to postulate such a mechanism. For the nickel peptides, we have presented evidence that both electron-transfer pathways are operative. The copper peptide self-exchange rate is unaffected by chloride,[8] even at $[Cl^-] = 0.1$ M. Thus, the nickel peptides react by an inner-sphere mechanism even more readily than the copper peptides, probably because of their higher affinity for axial substitution.

A further example of apparent inner-sphere electron transfer in nickel peptides is the reaction of $IrCl_6^{2-}$ with $Ni^{II}(H_{-2}Aib_3)^-$.[37] The rate constant for this reaction is too large to measure by stopped-flow methods but was determined by a pulsed-flow technique to be 5.8×10^7 M^{-1} s^{-1}. With use of the known $Ir^{IV,III}Cl_6^{2-,3-}$ self-exchange rate constant of 2.3×10^5 M^{-1} s^{-1},[38] its reduction potential of 0.892 V vs. NHE,[30] and a k_{11} value of 550 M^{-1} s^{-1} for $Ni^{III,II}(H_{-2}Aib_3)^{0,-}$, the rate constant for this reaction may be calculated as 3.5×10^4 M^{-1} s^{-1} from eq 2, which is derived with the assumption of an outer-sphere process. The large, 1000-fold discrepancy points to a more facile pathway such as formation of an axial chloride bridge.

Conclusion

Deprotonated peptide complexes of nickel(II) and nickel(III) have electron self-exchange rate constants that depend considerably on the structure of the complex. The nickel peptides fall roughly into three classes: $Ni^{III,II}(H_{-3}L)$, with $k_{11} \simeq 1.2 \times 10^5$ M^{-1} s^{-1}; $Ni^{III,II}(H_{-2}L)$ except Aib-containing peptides, $k_{11} \simeq 1.3 \times 10^4$ M^{-1} s^{-1}; the complexes of Aib_3 and $A(Aib)_2$, with $k_{11} \simeq 5.5 \times 10^2$ M^{-1} s^{-1}. The reasons why the rate constants for the Aib-containing tripeptide complexes are significantly smaller than the other doubly deprotonated complexes are not clear. However, it is possible that the electron-transfer reactions are enhanced for all the nickel–peptide complexes except those with Aib. The nature of the interaction causing the enhancement is not yet understood, but it would have to depend on the close approach of the complexes to each other, probably in the axial direction, which is blocked by the methyl groups in the Aib peptides. If this is the case, the apparent self-exchange rate constants would not be valid for reactants where the enhanced path is absent. While the k_{11} values are the observed self-exchange rate constants, they may not be the same as the outer-sphere self-exchange rate constants.

The electron-transfer reactions are catalyzed by bridging ligands such as Br^- and Cl^-, which can coordinate Ni(III) but are inhibited by nonbridging ligands like pyridine. In the presence of halides, the reactions follow both inner- and outer-sphere pathways.

Acknowledgment. We thank A. W. Hamburg for the synthesis of the Aib peptides. The Varian XL-200 spectrometer was purchased with funds from NSF Grant No. CHE-8004246. This investigation was supported by Public Health Service Grant Nos. GM19775 and GM12152 from the National Institute of General Medical Sciences.

Registry No. Br^-, 24959-67-9; Cl^-, 16887-00-6; N_3^-, 14343-69-2.

(30) Newton, M. *Int. J. Quantum Chem., Quantum Chem. Symp.* **1980**, *14*, 363.
(31) Bossu, F. P.; Chellappa, K. L.; Margerum, D. W. *J. Am. Chem. Soc.* **1977**, *99*, 2195.
(32) Linck, R. G. *MTP Int. Rev. Sci.: Inorg. Chem., Ser. One* **1971**, *9*, 303.
(33) Taube, H. *Ber. Bunsenges. Phys. Chem.* **1972**, *76*, 964.
(34) Owens, G. D.; Chellappa, K. L.; Margerum, D. W. *Inorg. Chem.* **1979**, *18*, 960.
(35) Owens, G. D.; Margerum, D. W. *Inorg. Chem.* **1981**, *20*, 1446–1453.
(36) Anast, J. M.; Margerum, D. W. *Inorg. Chem.* **1982**, *21*, 3494–3501.
(37) Owens, G. D.; Margerum, D. W. *Anal. Chem.* **1980**, *52*, 91A.
(38) Hurwitz, P.; Kustin, K. *Trans. Faraday Soc.* **1966**, *62*, 427.